ORIGINAL ARTICLE

lajss.org
Latin American Journal of Solids and Structures

www.lajss.org

Seismic fragility assessment of typical bridges in Northeastern Brazil

Gustavo Henrique Ferreira Cavalcante[a]*, Eduardo Marques Vieira Pereira[a], Isabela Durci Rodrigues[b], Luiz Carlos Marcos Vieira Júnior[a], Jamie Ellen Padgett[c], Gustavo Henrique Siqueira[a]

[a] Universidade Estadual de Campinas – Unicamp, Faculdade de Engenharia Civil, Arquitetura e Urbanismo, Departamento de Estruturas, Campinas, SP, Brasil. E-mail: ghenriquefc@hotmail.com, eduardo.marquesvp@gmail.com, vieirajr@unicamp.br, siqueira@fec.unicamp.br

[b] Universidade de São Paulo – USP, Escola de Engenharia de São Carlos, Departamento de Estruturas, São Carlos, SP, Brasil. E-mail: idrodrigues@usp.br

[c] Rice University – Department of Civil and Environmental Engineering, Houston, Texas, United States. E-mail: jamie.padgett@rice.edu

* Corresponding author

https://doi.org/10.1590/1679-78257062

Abstract

This paper presents a seismic fragility assessment of bridges commonly found in Northeastern Brazil. A generic three-dimensional nonlinear finite-element model is generated in OpenSees to enable variation of geometric features and component modeling. A parametric analysis is performed to evaluate the impact of the geometric and physical variations of the bridge inventory on the seismic behavior of the structures. Nonlinear time-history analyses using four sets of natural earthquake records are performed to obtain the Probabilistic Seismic Demand Model for the bridges. Capacity models are adopted according to previous studies to be combined with demand models to generate fragility functions. This article helps the decision markers to predict the seismic behavior of typical bridges in Northeastern Brazil, which enables the evaluation of risk mitigation methods.

Keywords

seismic demand, fragility functions, parametric analysis, earthquake engineering, vulnerability assessment

Graphical Abstract

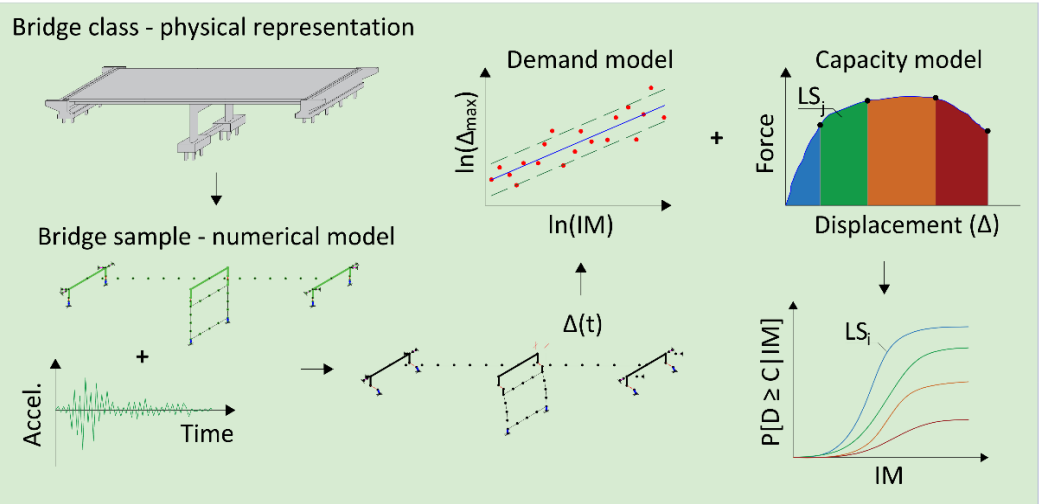

Received: March 26, 2022. In revised form: July 03, 2022. Accepted: July 25, 2022. Available online July 26, 2022.
https://doi.org/10.1590/1679-78257062

1 INTRODUCTION

Brazil is located in the mid-plate South America stable region, characterized by low seismic activity. Despite that, a considerable number of small-to-moderate events have occurred in the country. For instance, moment magnitude 5.0 earthquakes occur in Brazil on average every five years, and the largest recorded event amounts to 6.2 moment magnitude (Assumpção et al., 2016). Despite that, Brazilian earthquake-resistant design code (ABNT, 2021) applicable to bridges was only released in 2021, which implies that most of the bridges are likely not designed according to seismic-resistant provisions. As highlighted in Santos and Lima (2005) only special structures, such as Nuclear Power Plants, considered seismic provisions before 2006. This fact can be evidenced in typical Brazilian bridges with elastomeric bearings due the absence of earthquake-resistant measures, such as elastomeric isolation bearings, restrainer cables, seat extenders or shear keys. Note that some measures (e.g., increased reinforcement rates or use of steel jacket) increase column capacities, but to fully transfer horizontal loads to columns during earthquakes, it is necessary to restrain or limit excessive transverse motion to avoid unseating of bridge deck using restrainer cables or shear keys, for example. In this context, it is necessary to assess their vulnerability.

Fragility functions (FF) are important tools to assess the seismic vulnerability of a specific bridge or a class of bridges (Padgett and DesRoches, 2008), and typically represent the conditional probability of damage over a range of potential earthquake ground motion intensity. This damage potential is obtained from the convolution between the uncertain seismic demand and structural capacity. The seismic demand represents the structural response under ground excitation, whereas the capacity is the maximum response that a structure can withstand without exceeding a limit state or incurring a particular level of damage.

Analytical or simulation-based FF have been developed in regions where bridge damage records due to earthquakes are insufficient (Siqueira et al., 2014a), as in the case of the Brazilian territory. Several analytical fragility assessment studies in bridges were conducted worldwide, such as in the United States (Choi and Jeon, 2003; Padgett and DesRoches, 2009; Pahlavan et al., 2016; Mangalathu et al., 2017), Canada (Tavares et al., 2012; Siqueira et al., 2014a; Siqueira et al., 2014b), Japan (Karim and Yamazaki, 2003), Taiwan (Liao and Loh, 2004), South Korea (Lee et al., 2007), Greece (Moschonas et al., 2009) and Turkey (Avsar and Yakut, 2012). However, to the best of the authors' knowledge, no study has been carried out in Brazil. Therefore, the seismic performance of bridges countrywide remains unknown, as well as the sensitivity of this performance to the uncertainties involved.

To address the lack of understanding of relative performances of bridges in the region, a fragility assessment for bridge typologies commonly found in the Northeast region of Brazil is carried out in this paper. The Brazilian Northeast presents a relatively high seismic activity when compared to other parts of Brazil, as observed in Giardini et al. (1999), Assumpção et al. (2016) and Petersen et al. (2018). In Brazil, the National Department of Infrastructure and Transportation (DNIT) is responsible for supervising more than 5000 bridges on federal highways (Oliveira et al., 2019); and about half of these bridges are located in the Northeastern region of Brazil. This region comprises 9 states, an area of approximately 1552167 km^2, and it is the second most populous region in Brazil with a population of approximately 57.37 million (IBGE, 2010).

The fragility assessment carried out herein provides the basis for future regional risk analyses, while also shedding light on critical structural responses, important parameters across the portfolio, and distinguishing features of typical bridge classes in the region. These bridge class level demand analyses are particularly well suited for comparative assessment of the behavior of common bridge typologies, and for loss estimation. The subsequent sections of the paper present the bridge characteristics, modeling approach, and parametric analysis, followed by demand, capacity and fragility estimation.

2 BRIDGE CHARACTERISTICS

In Northeastern Brazil, DNIT is responsible for about 2500 bridges on national highways, which are inspected trough a management system denominated Sistema de Gestão de Obras de Arte Especiais (SGO). This system presents several survey reports that include bridge geometrical characteristics, inspection data, and structural rating information. Therefore, 250 bridge reports (about 10% of the total) are randomly collected to study their geometric and structural characteristics to properly group them into representative classes (Table 1). The authors considered the adoption of 250 survey an adequate compromise between the work of collecting more and having reasonable amount of data to analyze structural schemes and describe the geometric parameters by statistical tools.

Table 1 Representativeness and description of the bridge classes.

Bridge class	Bridge description	%
SS-SD-Abut	Single-span, slab deck and non-integral abutments	16.4%
SS-TB-Abut	Single-span, T-beam deck and non-integral abutments	27.6%
MSC-TB	Multi-span continuous, T-beam deck, two column bents and no abutments	17.2%
MSC-TB-Abut	Multi-span continuous, T-beam deck, two column bents and non-integral abutments	6.4%
Others		32.4%

Four representative bridge classes (i.e., SS-SD-Abut, SS-TB-Abut, MSC-TB and MSC-TB-Abut, as defined in Table 1) are studied to develop the FF, as the other individual classes, such as multi-span discontinuous bridges with elastomeric bearings and non-integral abutments, represented each less than 5% of the total summing up to 32.4% of the total (Bridge class Others in Table 1). Cast-in-place and straight concrete bridges supported on elastomeric bearings compose these representative classes. Figure 1 shows the geometric and structural characteristics of these classes. Note that two representative types of non-integral abutment (i.e., U seat-type and gravity seat-type abutments) are seen in the SS-TB-Abut and MSC-TB-Abut classes; however, each individual bridge has only one type.

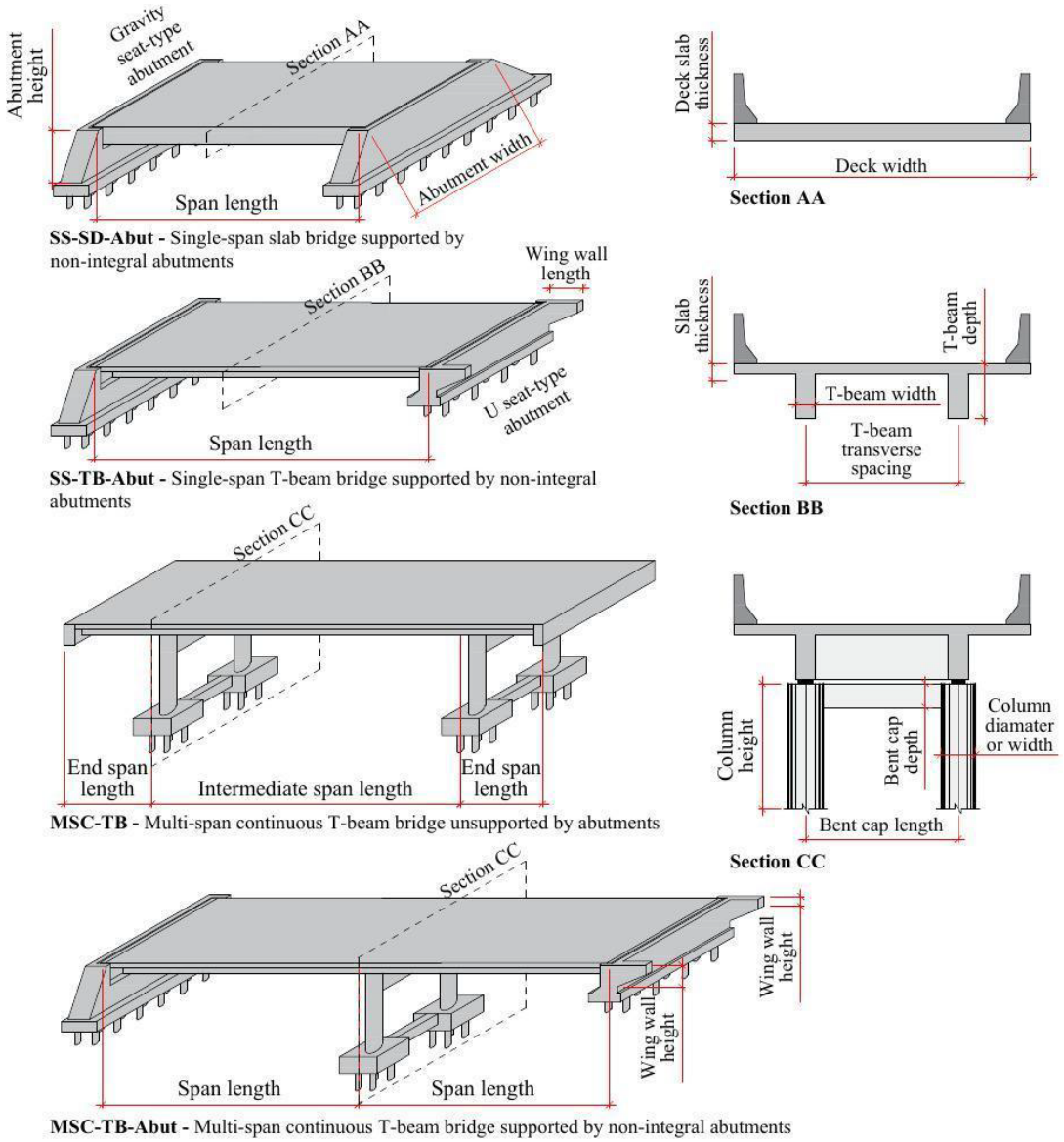

Figure 1 Geometric properties of the bridge classes.

From the reports, the geometric characteristics (e.g., number of spans, span length, column height, abutment height) are adjusted by discrete and continuous distributions, which allows bridge sampling to adequately consider bridge variability within each class. In addition, direct linear relations are established between parameters with strong correlations (i.e., Pearson's linear correlation coefficients greater than 0.7), such as span length and T-beams' depth. More details are available in (Cavalcante et al., 2021).

The foundations, material properties and design details are not available in the DNIT database, such as concrete strength (fc), steel yield stress (fy), steel Young's modulus (Es), damping ratio (ξ), abutment gap length (Gap) and elastomeric pads shear modulus (G). Table 2 illustrates the distributions adopted to describe these parameters. A C20 concrete class was assumed to represent the majority of the bridges, since most of them (about 78%) were built up to 1975 (Cavalcante et al., 2021). Finally, these continuous distributions are used to create different bridge samples.

Table 2 Material variability considered herein.

Variable	Distribution	Parameters	Reference
fc (MPa)	Normal	$\mu = 26.2$ and $\sigma = 4.3$	Santiago and Beck (2017)
fy (MPa)	Normal	$\mu = 576$ and $\sigma = 46.1$	Nogueira (2010)
Es (GPa)	Normal	$\mu = 200$ and $\sigma = 6.6$	Mirza and MacGregor (1979)
ξ (%)	Lognormal	$\lambda = 1.96$ and $\zeta = 0.18$	Siqueira et al. (2014a)
Gap (mm)	Normal	$\mu = 24.5$ and $\sigma = 5$	Tavares et al. (2012)
G (MPa)	Lognormal	$\lambda = -0.20$ and $\zeta = 0.14$	Siqueira et al. (2014a)

Brazilian bridges are expected to have non-seismic detailing (i.e., no shear keys, restrainer cables, elastomeric isolation bearing or steel jacket); therefore, a longitudinal reinforcement ratio of 1% is adopted for the columns (Padgett and DesRoches, 2009). In addition, transverse ties with diameters of **8 mm** and a spacing of **20 cm** are used in the columns according to the minimum requirements of ABNT (2014). The reinforcements of the bent caps are calculated based on the minimum requirements of ABNT (2014).

Bearing information is not available in the reports. Therefore, bearing designs are performed with a maximum service stress of 7 MPa, according to Kelly (1993). Four bearings per abutment are adopted in the SS-SD-Abut bridge class. SS-TB-Abut, MSC-TB and MSC-TB-Abut bridge classes have one bearing per T-beam on each support. MSC-TB bridge class has bearings only on the bents.

To properly classify the soil type and design the foundation of abutments and bents, 206 Standard Penetration Test (SPT) results from 61 different sites located in 22 cities in the target area are analyzed. Based on the results on the SPT data and considering the classification proposed in ASCE (2017), the soil on the region of the study is classified as stiff soil (site class D), since it represents 79% of the samples. Based on these SPT results, a typical soil defined as silty sand was adopted to estimate the parameters to model the abutments and the soil-structure interaction.

The design of the number of piles for each abutment depends on its type and geometry. Gravity seat-type abutments have greater pile cap lengths, which allows for an increase in the number of piles. U seat-type abutments have wing walls that change the distribution of transverse loads from lateral soil movement. The axial load capacity of the piles is calculated for each SPT, each pile with 10 meters length and 40 centimeters diameter. In addition, a group of four piles is considered as the maximum value to be adopted for the foundation of each column. The number of piles per foundation is defined based on the axial load capacity of the piles, considered as the mean value of 600 kN herein.

3 BRIDGE MODELING

The OpenSees analysis platform (McKenna, 2011) is used to create a generic finite-element (FE) model (Figure 2), which allows for variation in structural modeling (i.e., geometric characteristics, material properties, component modeling). The superstructure is modeled considering a single elastic beam-column element in the center of the deck cross section; since it is expected to remain essentially elastic under an earthquake (Choi and Jeon, 2003), as also done elsewhere by Liao and Loh (2004), Padgett and DesRoches (2009), Avsar and Yakut (2012), Siqueira et al. (2014a) and Mangalathu et al. (2017). Rigid-link beams are used in transverse and vertical directions on abutments and along the bridge piers to transfer lateral and gravitational loads from the deck to the transverse bent beams and abutments.

The bent beams and columns are modeled using fiber-type displacement-based beam-column elements with spread plasticity. The cross section of the element is divided into several fibers that delineate the regions of confined, unconfined concrete, and the longitudinal steel reinforcement. Uniaxial concrete and steel reinforcement material behavior are used

in OpenSees (i.e., Concrete07 and Steel02) based on the model proposed by Chang and Mander (1994) and Filippou et al. (1983), respectively, with an isotropic strain-hardening ratio of 5% for the steel's model. Each column is divided into several elements along their height with an approximate length of 50 centimeters, and each bent beam and grade beam is divided into 4 elements along their length.

Zero-length elements are used to model connections between the superstructure and bents. These elements represent the bearing behavior. The elastomeric pad material law is defined as a perfect elasto-plastic material model (Tavares et al., 2012), where the initial stiffness is calculated using the geometry of the pad. The yield force is used based on the frictional coefficient defined experimentally by Schrage (1981) and the gravitational loads.

The soil-structure interaction from the bents is considered by zero-length elements, defined by six compliance springs and dampers (for the six degrees of freedom) at pile cap level. The springs represent the load-deformation behavior of pile foundations. The model developed by Novak (1991) is used to estimate the response of a single pile, and it also reduces the stiffness when there is an interaction effect from the pile group. Further details can be found in Suescun (2010). Rayleigh damping is adopted in the dynamic analyses in the first and second vibration modes.

The bridge inventory has both Gravity and U seat-type abutments. The models for both abutment types are assumed to be the same, as described above. However, differences in the design of the number of piles and geometry generate different values of longitudinal and transverse stiffness. Zero-length elements are used to model connections between superstructure and abutments and impact elements (Figure 2). The gaps are modeled considering pounding between decks and abutments, which accounts for the energy dissipation during the contact, based on Muthukumar (2003). The abutments are assumed to be vertically rigid. Piles and soil backfill, through parallel springs, define the longitudinal contribution from the abutments. The soil backfill acts in passive loading of the abutment, while piles act in both active and passive directions. The abutments piles assume the tri-linear model implemented by Choi (2002), with Caltrans (California Department of Transportation, 2004) recommendations. The soil backfill is also modeled using a tri-linear model described in Nielson (2005) with Martin and Yan (1995), and Caltrans (California Department of Transportation, 2004) recommendations. The transverse contribution of the abutments includes only the piles, as Caltrans (California Department of Transportation, 2004) recommends that the resistance of the wing wall is neglected, which is also evidenced by the fact that most bridges classified as MSC-TB-Abut do not have structural elements to restrain the transverse displacements of the deck in the abutments. In addition, part of the MSC-TB bridges do not have wing walls. The abutment piles assume the same behavior in both directions.

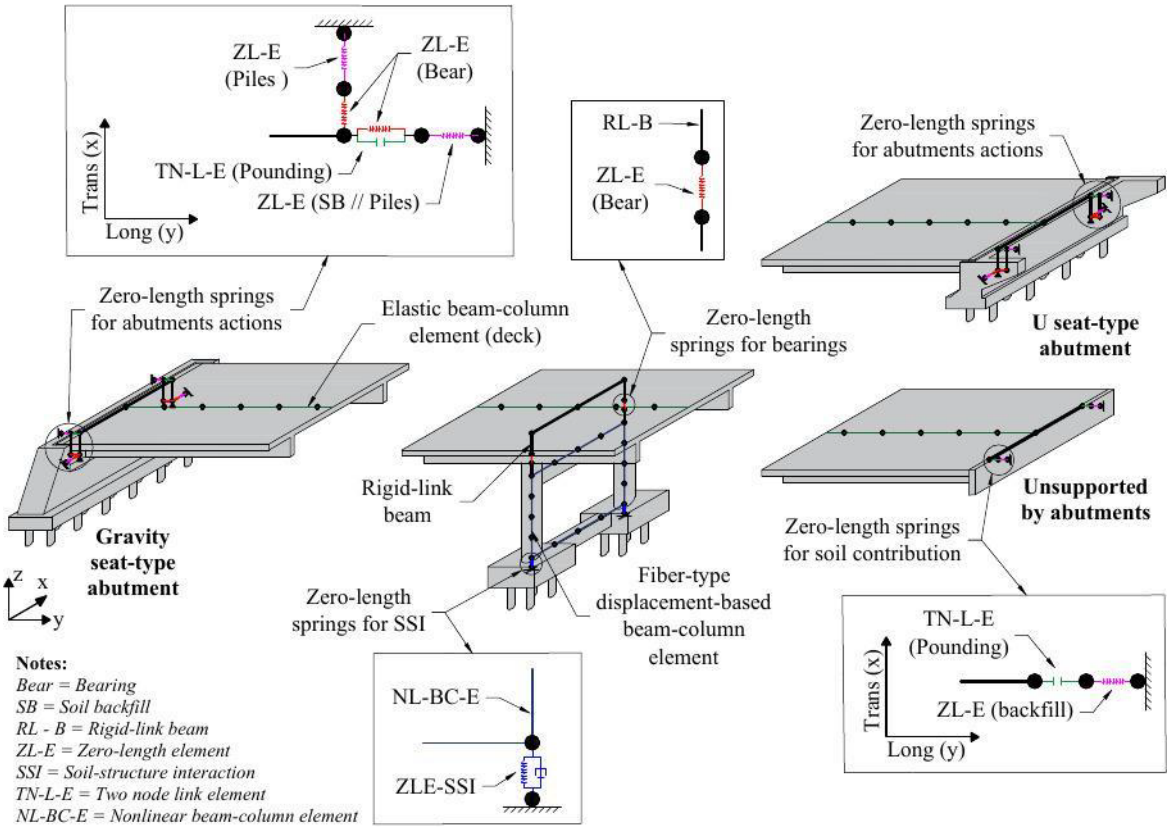

Figure 2 Generic FE model.

Bridges unsupported by abutments include the soil backfill contribution in longitudinal direction at the end spans. Vertical and transverse soil contributions are neglected. In these bridges, transverse and vertical forces are transferred from the deck to the bents through the elastomeric bearings.

4 GROUND-MOTION SUITE

In the absence of a database of filtered ground motion records for Brazil, 100 pairs of natural earthquake records are extracted from the Pacific Earthquake Engineering Research Center NGA-West2 database (PEER, 2021) to perform the dynamic analyses. The selected records were originated mainly from the strike-slip regime, which is compatible to the predominant source mechanism in Northeastern Brazil, as described by Bezerra et al. (2011). A minimum fault distance of 15 km is set to avoid near-fault ground motions (GM) (Medina and Krawinkler, 2004), and a maximum of 100 km is set to minimize regional attenuation effects (Stewart et al., 2013). Moment magnitudes in the 5.0 to 6.5 range are adopted as the maximum magnitude about one order larger than the largest event in the region, as suggested by Budnitz et al. (1997), and this range is consistent with seismic hazard studies for the region as seen in Petersen et al. (2018) and Souza et al. (2019). In order to consider the hazard variability in the region of interest, the above-mentioned parameters are divided into four bins: small-magnitude-small-distance (15-40 km, 5-5.7M), small-magnitude-large-distance (40-100 km, M5-5.7), large-magnitude-small-distance (15-40 km, M5.7-6.5), large-magnitude-large-distance (40-100 km, M5.7-6.5).

Figure 3 illustrates the 5%-damped spectrum and the geometric mean of each set of ground motions (GM), represented by 25 pairs of records (i.e., longitudinal and transverse directions) per bin.

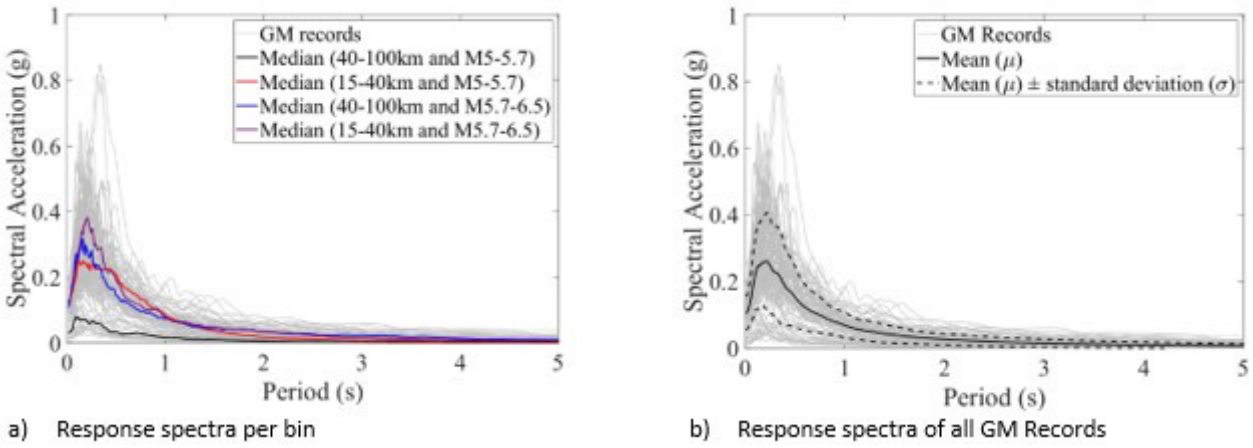

Figure 3 Response spectra of the ground motions with 5% damping.

5 PARAMETRIC ANALYSIS OF BRIDGE INVENTORY

When assessing the vulnerability of a portfolio of bridges it is necessary to consider the variability of different parameters that have an influence on the structural response of the bridges (Siqueira et al., 2014b). The bridge inventory presents variation in geometric parameters, such as span length and deck width, in addition to uncertainties in parameters used in bridge modeling, such as the steel yield strength and the concrete compressive strength. To discern which of these parameters should be treated explicitly as uncertain or could be assumed as a deterministic value when developing the probabilistic demand models, an analysis of variance (ANOVA) is conducted. Herein, a two-level fractional factorial design ($2_{IV}^{k-p} = 16$ runs) is performed using p-values generated from a Fisher test based on design-of-experiments (DOE) principles, as shown in Montgomery (2017). Only main effects are considered, since if the interaction between factors is significant, it means that at least one of them must also be significant (Wu and Hamada, 2009).

Nonlinear time-history analyses using statistical blocks are performed. The blocks are generated using the Latin-hypercube sampling (LHS) technique (Mckay et al., 1979), and one of their purposes is to avoid biasing the results from a single bridge geometry (Siqueira et al., 2014b). Eight geometry blocks are created per bridge class according to the results of the bridge inventory. The values of span length, deck width, column height and abutment height are variable (Table 3), except in the MSC-TB-Abut bridge class where the deck width value is constant. The individual influence of these parameters is not evaluated, since it is assumed that they have a strong influence on the structural behavior of the

bridge, as described in Padgett and DesRoches (2008), Tavares et al. (2012) and Siqueira et al. (2014b). However, the overall blocking effect is tested.

Table 3 Geometric configuration of each bridge class per block.

Block	SS-SD-Abut/SS-TB-Abut/MSC-TB/MSC-TB-Abut bridge classes (units in m)				
	Span length	Deck width	Abutment height	Column height	Lmr[1]
1	6.3/6.7/19/10.7	10/12/11.9/10	7.3/4.3/-/9.8	-/-/3.8/5.7	-/-/0.23/-
2	8.2/5.2/17.5/12.4	12/12/10.7/10	6.2/5.1/-/5.8	-/-/7.2/6.3	-/-/0.24/-
3	5.4/7.4/22.5/20.7	10/8/10.3/10	1.9/3.5/-/7.6	-/-/1.7/2.5	-/-/0.23/-
4	9.4/11.6/10.9/17.8	10/10/11/10	5.5/4.6/-/8	-/-/2.3/7.3	-/-/0.28/-
5	14.4/15.1/15.9/15.8	12/8/12.8/10	3.7/3.1/-/7.3	-/-/4.4/4.1	-/-/0.25/-
6	4.1/11.7/20.6/26.2	10/8/11.4/10	4.9/5.8/-/3.6	-/-/2.8/5.1	-/-/0.23/-
7	7.2/13.5/15.6/14	10/10/9.9/10	3/2.4/-/6.7	-/-/5.3/4.6	-/-/0.22/-
8	11.1/7.5/14/8.4	10/8/9.3/10	4.3/3.9/-/4.9	-/-/3.2/3.5	-/-/0.25/-

[1] Ratio between middle-span length and end-span length

To consider the ground motion uncertainties, one replicate per block is applied, with each replica using one pair of ground motion records. Two pairs of records (longitudinal and transverse directions) are collected from each set of ground motions defined in the previous section, totaling eight pairs of records.

The lower and upper values of each parameter evaluated are defined by the quantiles of 5% and 95% of their respective distribution, as shown in Table 4. These parameters are assumed qualitative (i.e., abutment type and column type) or quantitative (i.e., slab thickness and damping).

Table 4 Lower (-) and upper (+) values of the parameters considered in the analysis.

Parameter	SS-SD-Abut		SS-TB-Abut		MSC-TB		MSC-TB-Abut	
	Level		Level		Level		Level	
	(-)	(+)	(-)	(+)	(-)	(+)	(-)	(+)
Slab thickness (cm)	27	89	24	32	21	32	-	-
Damping (%)	5.3	9.4	5.3	9.4	5.3	9.4	5.3	9.4
Abutment gap (mm)	16	33	16	33	-	-	16	22
Bearing shear modulus (MPa)	0.65	1.03	0.65	1.03	0.65	1.03	0.65	1.03
Abutment type	-	-	U	Gravity	-	-	U	Gravity
Number of T-beams	-	-	2	4	-	-	-	-
T-beam depth (m)	-	-	0.58	1.93	1.31	2.09	0.80	2.53
Column diameter (m)	-	-	-	-	0.58	0.90	60	118
Column width (m)	-	-	-	-	0.57	1.04	-	-
Column cross-section type	-	-	-	-	Circular	Rectangular	-	-
Bent cap length (m)	-	-	-	-	5.3	8.0	4.50	5.13
Bent cap depth (m)	-	-	-	-	0.97	1.29	-	-
Number of spans	-	-	-	-	3	5	2	4

Engineering Demand Parameters (EDP) are monitored to evaluate the significance of each parameter, representing component responses of the bridge. They are deck unseating (Unseating), column curvature (Col), longitudinal and transverse displacements of the bearings (BearL and BearT), active, passive and transverse displacements of the abutments (AbutAct, AbutPass and AbutT), as adopted by Pahlavan et al. (2016) and Mangalathu et al. (2017). The deck unseating is an important EDP, as the bridge classes have elastomeric bearings without steel dowels, shear keys or other mechanism to restrain the transverse displacements of the deck when the bearing slides under seismic events. The p-values are presented for the parameters selected in Table 4 and for the blocks. A significance cutoff level of $\alpha = 0.05$ is used according to Nielson (2005) and Siqueira et al. (2014b), which means that the parameter variation is significant if the p-value is less than 0.05. The combined effect of the blocks with the record-to-record variability has the greatest impact on the component responses (p-value lower than 0.01) for all bridge classes. Therefore, only the results of the parameters illustrated in Table 4 are presented.

Table 5 presents the results of SS-SD-Abut bridge class. The variation in slab thickness is considered significant in all component responses, since it directly influences the mass of the deck. The stiffness of the bearings depends on the bearing shear modulus, which is a significant parameter in the deck unseating, in the bearing displacements and in the transverse displacements of the abutments. The damping variation is not significant in the analysis. Therefore, a fixed value for the damping can be adopted considering the ranges used in Table 4. The component responses in the longitudinal direction (BearL, AbutAct and AbutPass) are most impacted by the abutment gap, since after the gap closes the structural behavior changes.

Component responses of the SS-TB-Abut bridge class are shown in Table 5. The number of T-beams has a high impact on the deck unseating and on the transverse displacements of the bearing. The number of T-beams determines the number of elastomeric bearings, directly related with the transverse stiffness of the bridge. The abutment gap has a high impact on the longitudinal response of the bridge as seen in the previous bridge class. The abutment type and the slab thickness are not significant parameters for all bridge classes. The variation between the lower and upper values of the slab thickness is very small and its impact is neglected. The bearing shear modulus, damping and T-beam depth have a significant impact on some of the component responses (i.e., deck unseating and displacements of the bearings).

Table 5 Calculated p-values for SS-SD-Abut and SS-TB-Abut bridge classes.

Parameter	SS-SD-Abut/SS-TB-Abut p-values					
	Unseating	**BearL**	**BearT**	**AbutAct**	**AbutPass**	**AbutT**
Slab thickness	**0.01**/0.54	**0.01**/0.46	**0.01**/0.56	**0.01**/0.99	**0.01**/0.72	**0.01**/0.09
Damping	0.15/**0.02**	0.36/0.54	0.15/**0.02**	0.92/**0.05**	0.81/**0.03**	0.42/**0.05**
Abutment gap	0.19/**0.05**	**0.01**/**0.01**	0.20/**0.05**	**0.01**/**0.01**	**0.01**/**0.01**	0.26/0.06
Bearing shear modulus	**0.01**/**0.01**	**0.01**/**0.01**	**0.01**/**0.01**	0.78/0.08	0.82/0.05	0.04/0.41
Abutment type	-/0.89	-/0.81	-/0.86	-/0.86	-/0.86	-/0.46
Number of T-beams	-/**0.01**	-/**0.01**	-/**0.01**	-/0.92	-/0.99	-/**0.01**
T-beam depth	-/**0.01**	-/0.06	-/**0.01**	-/0.06	-/**0.02**	-/**0.01**

[1] Boldface numbers indicate significant parameters (p-value < 0.05)

Table 6 describes the results of the sensitivity analysis for MSC-TB bridge class. The bearing shear modulus is the most significant parameter for the deck unseating and the transverse bearing displacements with the highest impacts. The column cross-section and the column type are the only significant parameters for the column responses. The slab thickness is a significant parameter for all component responses, except for the columns. The number of spans has a greatest impact on the longitudinal displacements of the bearings and is not significant for the responses of the other components. The damping is significant only for the longitudinal displacements of the bearings. T-beam depth, bent cap geometry, compressive concrete strength and steel yield strength are not significant parameters for seismic analysis.

Table 6 Calculated p-values for MSC-TB and MSC-TB-Abut bridge classes.

Parameter	MSC-TB/MSC-TB-Abut p-values						
	Unseating	**Col**	**BearL**	**BearT**	**AbutAct**	**AbutP**	**AbuT**
Slab thickness	**0.04**/-	0.52/-	**0.01**/-	**0.03**/-	-/-	-/-	-/-
Damping	0.07/**0.01**	0.07/0.82	0.11/0.75	**0.03**/**0.01**	-/0.07	-/0.07	-/0.11
Abutment gap	-/**0.01**	-/0.47	-/**0.01**	-/**0.01**	-/**0.01**	-/**0.01**	-/**0.02**
Bearing shear modulus	**0.01**/**0.01**	0.63/**0.05**	0.28/0.19	**0.01**/**0.01**	-/0.99	-/0.92	-/**0.01**
Abutment type	-/0.47	-/0.07	-/0.11	-/0.50	-/**0.01**	-/**0.02**	-/**0.01**
T-beam depth	0.75/**0.02**	0.81/0.10	0.54/0.77	0.82/**0.03**	-/0.65	-/0.84	-/0.03
Dimensions of the column cross-section	0.28/0.82	**0.01**/**0.01**	**0.01**/0.89	0.75/0.92	-/0.56	-/0.63	-/0.57
Column cross-section type	0.84/-	**0.01**/-	0.36/-	0.45/-	-/-	-/-	-/-
Bent cap length	0.79/0.06	0.89/0.43	0.99/0.17	0.77/0.06	-/0.99	-/0.72	-/**0.03**
Bent cap depth	0.61/-	0.81/-	0.84/-	0.65/-	-/-	-/-	-/-
Number of spans	0.44/**0.03**	0.73/0.77	**0.01**/0.19	0.44/**0.03**	-/**0.01**	-/**0.01**	-/0.26
Compressive concrete strength	0.62/0.86	0.24/0.40	0.92/0.99	0.82/0.79	-/0.89	-/0.99	-/0.41
Steel yield strength	0.86/0.32	0.82/0.99	0.43/0.65	0.73/0.34	-/0.09	-/0.07	-/0.07

[1] Boldface numbers indicate significant parameters (p-value < 0.05)

Table 6 also presents the results of the sensitivity analysis for the MSC-TB-Abut bridge class. Abutment gap has the highest impact on the component's responses in the longitudinal direction (i.e., bearings and abutments). Bearing shear modulus has a high impact on the deck unseating and on the bearing and abutment displacements in the transverse direction. The damping, the T-beam depth, the bent cap length and the number of spans are not the parameters with the greatest impact, but they are significant for some component responses. The abutment type is significant for the abutment responses, since different assumptions are assumed for the design of the number of piles per abutment type.

The variation of the damping is not significant for the SS-SD-Abut class. Therefore, a constant value is adopted as 7.07% for this class. The abutment type is not significant for the SS-TB-Abut bridge class, so gravity seat-type abutments are adopted for this class with new values of mean (μ = 4.49 m) and standard deviation (σ = 1.62 m) for the abutment height, considering all the abutments. The variation in slab thickness is also not significant for the SS-TB-Abut bridge class and a constant value of 0.28 is adopted for the seismic analysis. For the MSC-TB bridge class, the values of the T-beam depth, the bent cap length and the bent cap depth are assumed to be constant and equal to 1.7 m, 6.5 m and 1.1 m, respectively. For the MSC-TB and MSC-TB-Abut bridge classes, the values of the compressive concrete strength and the steel yield strength are assumed constant and equal to 26 MPa and 576 MPa, respectively.

Overall, the findings of this parameter study shed light on the importance of further in situ investigations of significant parameters that have been adopted by literature (e.g., damping and bearing shear modulus) and may not adequately represent the characteristics of existing bridges. Given the new insights on the significant parameters whose variation affects the seismic response of typical bridge classes in Northeastern Brazil, probabilistic estimates of the demand are pursued in the next section for these unique classes of bridges.

6 DEMAND ESTIMATES

Fragility assessment requires an analysis of seismic demand, given the level of intensity measure (IM). This section provides the first probabilistic seismic demand analysis of bridge classes in Northeastern Brazil, and hence leverages an established approach and model form for the bridge classes and components in the region. Emphasis is instead placed on testing the validity of this model form and insights gained from comparative analysis of these unexplored bridge classes. The seismic demand is estimated by cloud analysis, considering both record-to-record variability and epistemic uncertainties arising from geometric and mechanical properties. Cloud analysis has been widely used in bridge fragility assessment, as adopted in Choi and Jeon (2003), Padgett and DesRoches (2008), Siqueira et al. (2014a), Pahlavan et al. (2016) and Mangalathu et al. (2017). Furthermore, a power-law relation ($S_D = a \times IM^b$) is adopted (Luco and Cornell, 2007), where S_D is the median of the seismic demand, assumed to be lognormally distributed. The parameters of the probabilistic seismic demand model are estimated through a linear regression analysis of peak demand values relative to the intensity measure in the logarithmic space, where a linear relation between S_D and IM can be established (Equation 1), with *a* and *b* as regression coefficients.

$$ln\,(S_D) = ln\,(a) + b \times ln\,(IM) \tag{1}$$

Additionally, the logarithmic standard deviation of the demand ($\beta_{D|IM}$), conditional on the IM, is estimated as shown in Equation 2.

$$\beta_{D|IM} \cong \sqrt{\frac{\sum [ln\,(d_i) - ln\,(a \times IM^b)]^2}{N-2}} \tag{2}$$

where N is the number of simulations and d_i is the peak demand of the component of interest.

For the analyses, 100 samples per bridge class are generated using the LHS technique, which accounts for the uncertainties in the bridge geometry, material properties, and other random variables. The LHS is used to create a set of nominally identical but statistically different bridge samples. Each bridge sample is analyzed with a pair of ground motions by nonlinear time history analyses, amounting to 100 simulations per bridge class. In each simulation, the peak value for each monitored EDP is recorded.

6.1 IM Selection

The appropriate intensity measure (IM) should be examined according to several characteristics: proficiency (ζ), efficiency (βD|IM), practicality (b), sufficiency, relative sufficiency measure (RSM) and hazard computability (Padgett et al., 2008; Jalayer et al., 2012). Petersen et al. (2018) developed hazard curves for South America using PGA, $S_{a\text{-}0.2}$ and $S_{a\text{-}1.0}$; therefore, only these intensity measures are compared in terms of the aforementioned criteria. Other IMs are neglected

based on hazard computability criterion, since the next step in a risk assessment is the combination of the fragility with hazard curves or available probabilistic seismic hazard estimates. Furthermore, peak ground acceleration (PGA) and spectral acceleration at 1 second ($S_{a\text{-}1.0}$) have been widely used to develop FF for bridge portfolios, although region characteristics and design details have impact on appropriate IM selection (Choi and Jeon, 2003; Padgett and DesRoches, 2008; Tavares et al., 2012; Mangalathu et al., 2017). Figure 4 illustrates the proficiency results for each component with PGA and $S_{a\text{-}1.0}$ as IM; only these two IMs are depicted since they are the most commonly used IMs, and also performed better than $S_{a\text{-}0.2}$. Overall, PGA is a less proficient IM than $S_{a\text{-}1.0}$ according to Figure 4, since ζ is lower for all components.

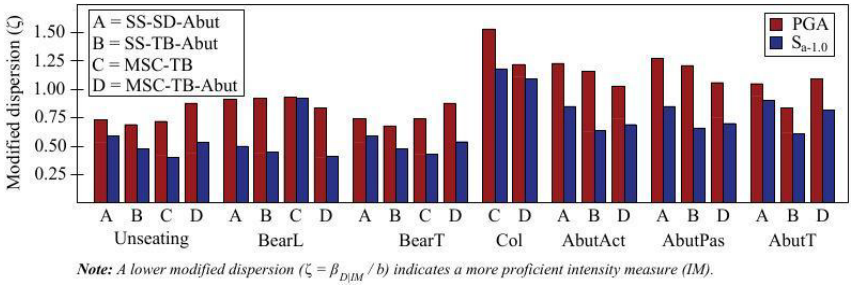

Figure 4 Results of proficiency of PGA and $S_{a\text{-}1.0}$ for each component.

Figure 5 shows the results of sufficiency of PGA and $S_{a\text{-}1.0}$ for each component. An IM is considered to be insufficient when the p-value is less than a threshold level such as 0.1 as adopted herein and in related studies (Padgett et al., 2008). PGA is conditionally statistically dependent on the magnitude of ground motions for most analyses (Figure 5). PGA is statistically independent on the distance of ground motions; however, $S_{a\text{-}1.0}$ is a more sufficient IM in 36 of 46 analyses. Furthermore, the RSM results indicated that $S_{a\text{-}1.0}$ is more sufficient than PGA for all analyses. Finally, $S_{a\text{-}1.0}$ is adopted as IM.

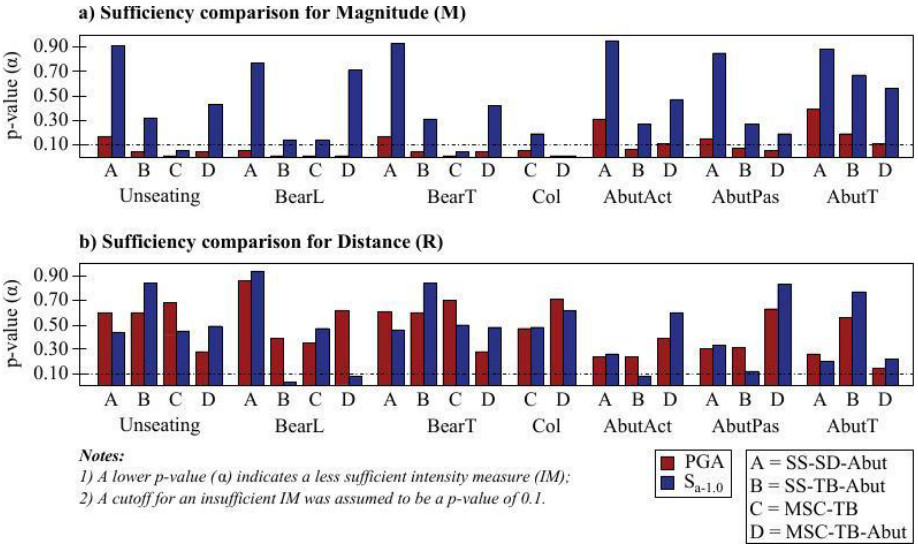

Figure 5 Results of sufficiency of PGA and $S_{a\text{-}1.0}$ for each component.

6.2 Probabilistic Seismic Demand Models

Using Equations 1 and 2, the results of the Probabilistic Seismic Demand Model (PSDM) are presented in Table **7**, which includes the median, dispersion and R-squared (R^2) for the components of each bridge class. The R-squared results indicate that the power law may not be a good fit for the column and abutment demand models. The trend of higher dispersion values for the abutment fit is also observed in Nielson and DesRoches (2007a), who used the same constitutive laws for modeling the abutments and gaps. The dispersion values obtained in the column demand fit are high due to the geometric variations of the bridge classes (i.e., column height and column diameter), as seen in Table 4.

Demand linear regressions in logarithmic space are also performed assuming a bilinear trend, as detailed in Jeon et al. (2015). This approach aims to account for the nonlinear behavior of the structural demand as the IM level increases, and provide more reliable estimates. Therefore, Figure 6a illustrates the column curvature results for the MSC-TB-Abut bridge class using linear and bilinear trends, where the break point is calculated to minimize the root mean squared error (RMSE). Slopes in bilinear regressions can vary significantly when compared to linear regressions (Figure

6a). A minimum number of points should be used in the linear regression of each branch (Figure 6b) to avoid unrealistic branches, such as with negative slopes. The results show that the RMSE value for the linear trend is 0.93 and for the bilinear trend is 0.90 (i.e., using 60% and 40% of the data to fit each branch, as seen in Figure 6b), which indicates a low reduction of approximately 3.2%. Similar results were observed for the other components and, for this reason, it is assumed that a linear trend is a good fit for the PSDMs presented in Table 7.

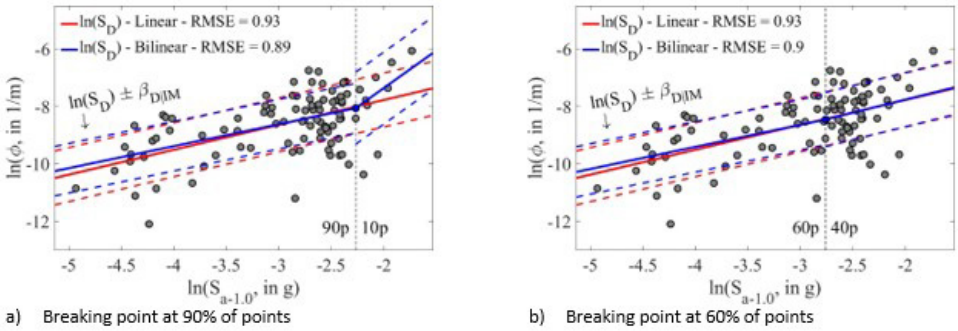

Figure 6 Comparison between linear and bilinear PSDMs of column curvature for MSC-TB-Abut bridge class.

The results (i.e., regression coefficients) indicate that the demand is greater for bridges with multiple continuous spans, as there are decks with greater mass mobilized during an earthquake. Single-span bridges commonly present lower fragility, which are often neglected. Nevertheless, these bridges must be evaluated as they represent around 40% of the total and can represent a significant seismic risk because of the relatively high exposure. Demands for deck and transverse bearing displacements are higher in the MSC-TB bridge class, as expected due to the lack of abutment systems; however, the soil backfill contribution in longitudinal direction reduces the demand for the bearing longitudinal displacements due to the absence of longitudinal gaps. The median values of transverse displacements are generally lower than longitudinal displacements of the abutments, since the inertial forces are transferred to the abutments in transverse direction only by the elastomeric bearings.

Table 7 PSDM for the typical bridges in Northeastern Brazil.

Bridge class	Demand parameter	ln(a)	b	$\beta_{D\|IM}$	R^2
SS-SD-Abut: Single-span slab bridge supported by non-integral abutments	Deck unseating (δ, in mm)	5.07	0.82	0.49	0.61
	Elastomeric bearing, longitudinal (δ, in mm)	5.12	0.87	0.43	0.69
	Elastomeric bearing, transverse (δ, in mm)	5.04	0.82	0.49	0.61
	Abutment, active (δ, in mm)	1.64	0.84	0.71	0.43
	Abutment, passive (δ, in mm)	1.64	0.84	0.72	0.43
	Abutment, transverse (δ, in mm)	1.42	0.75	0.68	0.40
SS-TB-Abut: Single-span T-beam bridge supported by non-integral abutments	Deck unseating (δ, in mm)	5.22	0.84	0.40	0.70
	Elastomeric bearing, longitudinal (δ, in mm)	5.19	0.86	0.39	0.73
	Elastomeric bearing, transverse (δ, in mm)	5.16	0.84	0.40	0.70
	Abutment, active (δ, in mm)	1.53	0.82	0.53	0.56
	Abutment, passive (δ, in mm)	1.56	0.83	0.55	0.55
	Abutment, transverse (δ, in mm)	1.61	0.81	0.50	0.59
MSC-TB: Multi-span continuous T-beam bridge unsupported by abutments	Deck unseating (δ, in mm)	5.56	0.88	0.35	0.78
	Column curvature (ϕ, in rad/m)	-6.47	0.83	0.86	0.28
	Elastomeric bearing, longitudinal (δ, in mm)	3.81	0.84	0.77	0.39
	Elastomeric bearing, transverse (δ, in mm)	5.47	0.87	0.37	0.75
MSC-TB-Abut: Multi-span continuous T-beam bridge supported by non-integral abutments	Deck unseating (δ, in mm)	5.31	0.82	0.44	0.65
	Column curvature (ϕ, in rad/m)	-6.04	0.87	0.94	0.31
	Elastomeric bearing, longitudinal (δ, in mm)	5.50	0.90	0.37	0.76
	Elastomeric bearing, transverse (δ, in mm)	5.26	0.81	0.44	0.65
	Abutment, active (δ, in mm)	2.44	1.01	0.69	0.53
	Abutment, passive (δ, in mm)	2.51	1.04	0.72	0.53
	Abutment, transverse (δ, in mm)	1.93	0.85	0.69	0.45

The PSDM results are used to derive fragility models (i.e., demand combined with capacity) for bridge classes typical of the region. Therefore, the next section describes the capacity models adopted to estimate FF.

7 CAPACITY ESTIMATES

The limit states of each component are defined following FEMA (1997), which characterizes four damage states: Slight, Moderate, Extensive and Complete Damage. The bridge deck (unseating), columns (col), abutments (AbutA, AbutP and AbutT) and bearings (BearL and BearT) are considered as components.

Column and deck unseating are considered the only components for extensive and complete damage, because at this level of damage it may lead to closure of the bridge, while the other components did not have noticeably effects on the vertical stability of the bridge at higher levels of damage (Pahlavan et al., 2016). The quantitative values of the damage states for the structural capacity of abutments, decks and bearings are obtained from Mangalathu et al. (2017). The structural capacity of columns is obtained from the multidirectional pushover analyses conducted by Cavalcante et al. (**2023**). The limit state capacities for each bridge component is depicted in Table 8.

Table 8 Bridge component limit state capacities.

Component	Slight		Moderate		Extensive		Complete	
	S_C	β_C	S_C	β_C	S_C	β_C	S_C	β_C
Deck unseating (mm)	-	-	-	-	152	0.35	229	0.35
Column curvature (rad/m)	0.009	0.63	0.015	0.56	0.024	0.68	0.036	0.69
Elastomeric bearing, longitudinal (mm)	25	0.35	76	0.35	-	-	-	-
Elastomeric bearing, transverse (mm)	25	0.35	76	0.35	-	-	-	-
Abutment, active (mm)	38	0.35	102	0.35	-	-	-	-
Abutment, passive (mm)	76	0.35	254	0.35	-	-	-	-
Abutment, transverse (mm)	25	0.35	102	0.35	-	-	-	-

8 FRAGILITY RESULTS

Fragility functions (FF) represent the conditional probability of a limit state (LS) exceedance, or that the seismic demand (D) exceeds the structural capacity (C), depending on the intensity measure (IM). Under the assumption that D and C follow lognormal distributions, a closed-form solution (Choi and Jeon, 2003) for the bridge-component fragility can be used (Equation 3):

$$P[LS|IM] = P[D \geq C|IM] = \Phi\left[\frac{\ln(S_D/S_C)}{\sqrt{\beta_{D|IM}{}^2+\beta_C}}\right] \quad (3)$$

The bridge-component fragility curves indicate the most vulnerable component of the system; however, the bridge-level fragility is greater than bridge-component fragilities (Nielson and DesRoches, 2007b).The bridge system level fragility is derived by estimating a Joint Probabilistic Seismic Demand Model (JPSDM) to capture the correlated demand on components and compare to capacity estimates. Given the adoption of a series system approximate, the probability that the system is at or beyond a particular limit state (FAILsystem) is the union of the probabilities of each component being in that same limit state (FAILcomponent-i), as seen in Equation 4. A detailed description is presented in Nielson and DesRoches (2007b).

$$P\left[FAIL_{system}\right] = \cup_{i=1}^{n} P[FAIL_{component-i}] \quad (4)$$

Table 9 depicts the values of the median (Med in units of g) and the dispersion (Disp) of the components' and system's fragility curves for each bridge class. Deck unseating and elastomeric bearings are the most vulnerable components in all bridge classes, except in the MSC-TB bridge class, where the soil backfill contribution reduces the longitudinal displacements of the bearings. The median values suggest that the columns and abutments are the least vulnerable components of the bridge classes. The abutments in longitudinal direction have the inertial forces of the deck transferred by elastomeric bearings and by the impact of closing the gap, increasing their vulnerability. The soil backfill

contribution, nevertheless, reduces the vulnerability of the passive direction of the abutments, which makes it the least vulnerable component in all bridge classes.

The deck unseating and the bearings considerably influence the system fragilities, since they are the most vulnerable components. Note that the MSC-TB and MSC-TB-Abut system fragilities for extensive and complete damage are equal to the deck unseating fragility functions, which indicates that the influence of the column fragility in these cases is not significant, hence the assumption made for the reinforcement ratio does not influence the results considerably. The MSC-TB is the class most vulnerable to higher damage states, since it has the highest probability of exceedance for the extensive and complete damage among the bridge classes. Abutments do not support this class and, therefore, the unseating of the bridge is expected to be more critical than other classes. The MSC-TB-Abut is the class most vulnerable to slight and moderate damage, since the MSC-TB bridge class has no gaps reducing the seismic demand in longitudinal direction. Single span bridge classes have less fragility than span lengths than multiple span bridge classes, as expected from demand results. Therefore, the SSD-SD-Abut and SS-TB-Abut are the least vulnerable classes, as expected according to FHWA (1995) and AASTHO (2007).

Table 9 Component and system FF for the typical bridges in Northeastern Brazil.

Bridge class	Component	Slight		Moderate		Extensive		Complete	
		Med	Disp	Med	Disp	Med	Disp	Med	Disp
SS-SD-Abut: Single-span slab bridge supported by non-integral abutments	Deck unseating	-	-	-	-	0.94	0.73	1.55	0.73
	Elastomeric bearing, longitudinal	0.11	0.64	0.40	0.64	-	-	-	-
	Elastomeric bearing, transverse	0.11	0.73	0.42	0.73	-	-	-	-
	Abutment, active	10.9	0.95	35.6	0.95	-	-	-	-
	Abutment, passive	24.8	0.95	104	0.95	-	-	-	-
	Abutment, transverse	10.8	1.02	69.9	1.01	-	-	-	-
	System	0.08	0.62	0.31	0.62	0.94	0.73	1.55	0.73
SS-TB-Abut: Single-span T-beam bridge supported by non-integral abutments	Deck unseating	-	-	-	-	0.80	0.64	1.30	0.64
	Elastomeric bearing, longitudinal	0.10	0.61	0.37	0.61	-	-	-	-
	Elastomeric bearing, transverse	0.10	0.64	0.36	0.64	-	-	-	-
	Abutment, active	12.9	0.77	43.0	0.77	-	-	-	-
	Abutment, passive	27.7	0.78	117	0.78	-	-	-	-
	Abutment, transverse	7.2	0.75	40.0	0.75	-	-	-	-
	System	0.08	0.56	0.28	0.56	0.80	0.64	1.30	0.64
MSC-TB: Multi-span continuous T-beam bridge unsupported by abutments	Deck unseating	-	-	-	-	0.54	0.56	0.87	0.56
	Column curvature	11.0	1.46	22.2	1.41	42.3	1.50	73.7	1.51
	Elastomeric bearing, longitudinal	0.49	1.01	1.85	1.01	-	-	-	-
	Elastomeric bearing, transverse	0.08	0.59	0.27	0.59	-	-	-	-
	System	0.07	0.59	0.27	0.58	0.54	0.56	0.87	0.56
MSC-TB-Abut: Multi-span continuous T-beam bridge supported by non-integral abutments	Deck unseating	-	-	-	-	0.71	0.68	1.16	0.68
	Column curvature	4.67	1.31	8.42	1.26	14.5	1.34	23.1	1.35
	Elastomeric bearing, longitudinal	0.08	0.56	0.27	0.56	-	-	-	-
	Elastomeric bearing, transverse	0.08	0.69	0.32	0.69	-	-	-	-
	Abutment, active	3.26	0.77	8.63	0.77	-	-	-	-
	Abutment, passive	5.82	0.77	18.6	0.77	-	-	-	-
	Abutment, transverse	4.59	0.91	24.2	0.91	-	-	-	-
	System	0.06	0.56	0.22	0.55	0.71	0.68	1.16	0.68

The system FF for each bridge class are depicted in Figure 7. FF can be used to estimate conditional LS exceedance probabilities according to specific return periods (RP). This approach allows for an assessment of fragility for a target hazard, which is commonly adopted in seismic design codes. As an application, Petersen et al. (2018) developed and made available hazard maps for South America with RPs of 72, 475 and 2475 years. These maps enable collection of the maximum values of $S_{a\text{-}1.0}$ (site class B) in Northeastern Brazil for each RP. These acceleration values are adjusted for stiff soil (site class D) to properly account for site amplification factors using ASCE (2017) coefficients. Table 10 presents the

results of conditional LS exceedance probabilities for the bridge classes according to the maximum values of $S_{a\text{-}1.0}$ for each RP in the entire region.

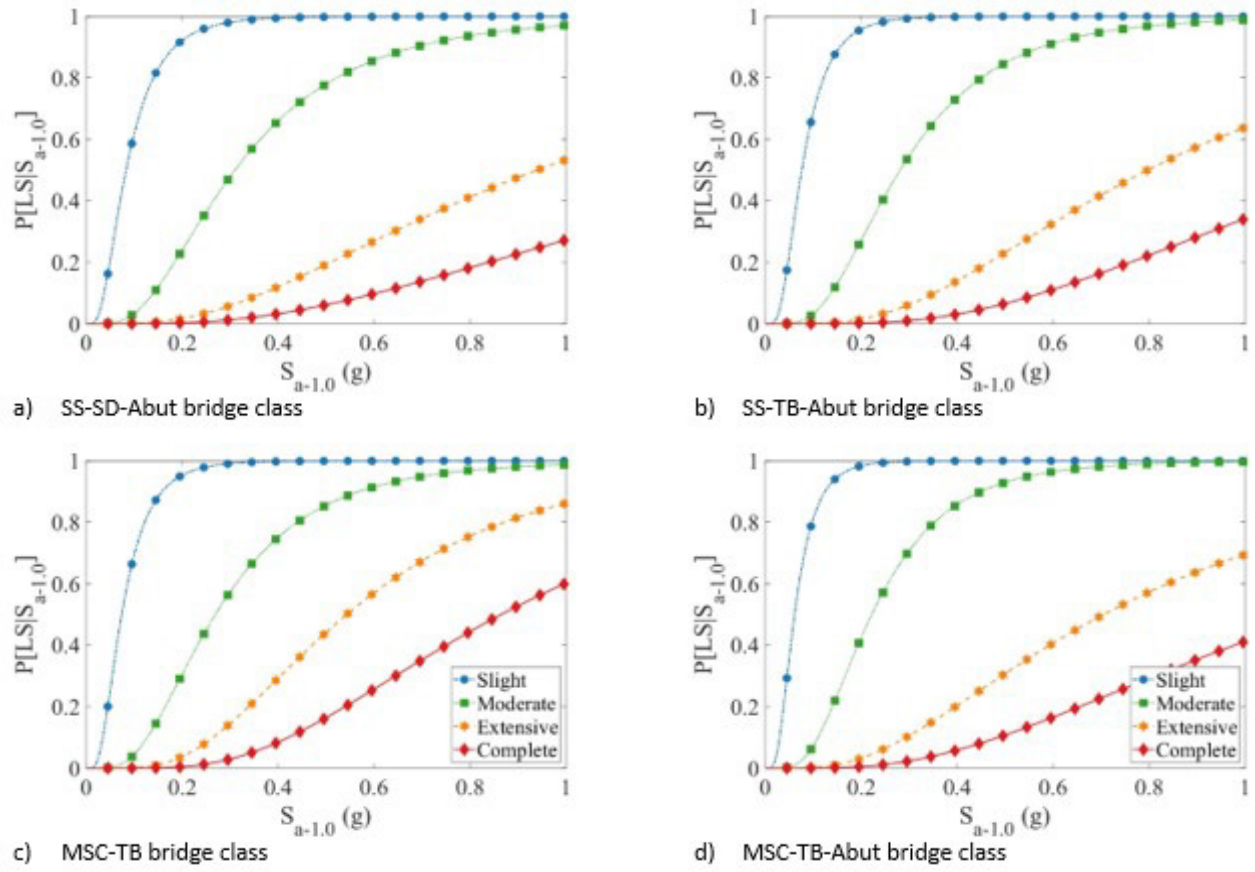

Figure 7 System fragility curves for the bridge classes.

Conditional LS exceedance probabilities for expected accelerations in a 72-y RP (i.e., 0.04 g) are not significant for extensive and complete damage; however, probabilities for slight damage are up to 23.45%, while moderate damage can reach 0.10%. When the RP is increased from 72 to 475 years, the accelerations increase about three times (from 0.04 g to 0.19 g) and the probabilities over 400 times. For a RP of 2475 years, the probabilities for slight, moderate, extensive and complete damage are up to 99.99%, 93.22%, 44.53% and 16.13%, respectively. These probabilities must be evaluated by the stakeholders to assess the need for safety measures (i.e., retrofit).

Table 10 Component and system FF for the typical bridges in Northeastern Brazil.

Bridge class	Return period (years)	$S_{a\text{-}1.0}$	$P[LS\|S_{a\text{-}1.0}]$ (%)			
			Slight	Moderate	Extensive	Complete
SS-SD-Abut	72	0.04 g	13.18	0.05	0.00	0.00
	475	0.19 g	91.85	21.49	1.43	0.20
	2475	0.50 g	99.84	77.97	19.36	6.06
SS-TB-Abut	72	0.04 g	10.79	0.03	0.00	0.00
	475	0.19 g	93.87	24.43	1.23	0.13
	2475	0.50 g	99.95	84.98	23.14	6.77
MSC-TB	72	0.04 g	17.14	0.06	0.00	0.00
	475	0.19 g	95.47	27.57	3.11	0.33
	2475	0.50 g	99.96	85.18	44.53	16.13
MSC-TB-Abut	72	0.04 g	23.45	0.10	0.00	0.00
	475	0.19 g	98.02	39.49	2.76	0.39
	2475	0.50 g	99.99	93.22	31.04	10.79

There are some limitations to the results presented in Table 10. For example, these estimated accelerations are likely to be overestimated, as the location where the Sa-1.0 values where collected may not have bridges. In addition, this study provides an estimate of a regional vulnerability, which may not be representative for specific bridges; therefore, these insights should be treated as a preliminary indication of expected global behavior and potential screening tool for vulnerable bridges.

9 CONCLUSION

This paper presents a first fragility assessment for typical bridges in Northeastern Brazil, which is based on a detailed study of the geometric and structural variation of this group of bridges. Therefore, several analyses are performed to provide a reliable estimate of the bridge inventory's vulnerability, as an essential and new contribution to future studies on seismic risk analyses in the region.

A parametric analysis is performed to evaluate the impact of the geometric and physical variations of the bridge inventory on the seismic behavior of the bridge classes. Variations in span length, deck width, column height and abutment height, and record-to-record variability have a high impact on seismic demand, while variations in some parameters (e.g., bent cap depth and compressive concrete strength) are not significant. This allows estimating which parameter variations do not require further investigation, and which should be defined by on-site investigations or via probability distributions based on literature recommendation.

Fragility functions are derived based on demand and capacity models. While the capacity models are estimated based on literature recommendations, emphasis is placed on understanding the distinct seismic response of bridges in the region. Demand is assessed by PSDMs, which are based on long-period spectral acceleration, as it performed better than other IMs. A systematic study and selection of an optimal IM provides insights into the degree of uncertainty in the demand results. Demand models for regional bridge inventories provide essential information about the behavior of key components (e.g., bearings) in a vulnerability assessment, which includes particular characteristics of the structures.

According to the **fragility function** results, deck unseating and bearings are the most vulnerable components in all of the bridge classes, while the columns and abutments are the least vulnerable components. The MSC-TB is the class most vulnerable to higher levels of damage. However, the MSC-TB-Abut is the class most vulnerable to slight and moderate damage, since the MSC-TB bridge class has no gaps which reduces the seismic demand in longitudinal direction. The single span bridge classes (SS-SD-Abut and SS-TB-Abut) have shorter span lengths than multiple span bridge classes, contributing to their relatively lower vulnerability.

An example of application of **fragility functions** combined with target hazards indicates that conditional LS exceedance probabilities can be estimated for different **return periods**. These probabilities are reasonable estimates of the structural safety of the bridge inventory, which can be associated with acceptance criteria (e.g., reliability indices) to assess the need for retrofit measures by stakeholders. In addition, these FF can be associated with exposure and hazard models to derive estimates of direct and indirect losses from earthquakes.

As this is the first of its kind study conducted for Brazil, it is important to acknowledge some limitations in order draw a path for future studies. Regarding the inventory, in-situ investigations can provide valuable information on the elastomeric bearings (e.g., geometry and quality), given the importance of this component in the structural response. When comprehensive hazard studies become available, rigorous ground motion selection procedures should be used to review the results.

The authors gratefully acknowledge the financial support of the Coordenação de Aperfeiçoamento de Pessoal de Nível Superior - Brasil (CAPES) - Finance Code 001; the National Council for Scientific and Technological Development - CNPq (Process # 308040/2021-0); and the São Paulo Research Foundation (FAPESP) - Finance Code 2018/23304-9. The opinions, findings, and conclusions or recommendations expressed in this paper are those of the authors only and do not necessarily reflect the views of the sponsors or affiliates.

Author's Contributions: Conceptualization, GHF Cavalcante; Data curation, GHF Cavalcante; Methodology – GHF Cavalcante, EMV Pereira and ID Rodrigues; Formal analysis – GHF Cavalcante, EMV Pereira, IR Rodrigues, JE Padgett and GH Siqueira; Software – GHF Cavalcante; Writing – original draft – GHF Cavalcante, EMV Pereira and ID Rodrigues; Project administration – LCM Vieira Junior and GH Siqueira; Writing – review & editing – JE Padgett and GH Siqueira; Supervision – GH Siqueira.

Editor: Marco L. Bittencourt

References

AASTHO LRFD (2007), Standard specifications for highway bridges. U.S.

American Society of Civil Engineering (2017), ASCE 7-16: Minimum design loads and associated criteria for buildings and other structures.

Assumpção, M., Pirchiner, M., Dourado, J. and Barros, L. (2016), "Terremotos no Brasil: preparando-se para eventos raros", Boletim SBGf, 96(1), 25-29.

Associação Brasileira de Normas Técnicas (2021), NBR 7187: Design of concrete bridges, viaducts and footbridges. Rio de Janeiro, RJ, Brazil: ABNT.

Associação Brasileira de Normas Técnicas (2014), NBR 6118: Design of concrete structures - Procedure. Rio de Janeiro, RJ, Brazil: ABNT.

Avsar, O. and Yakut, A. (2012), "Seismic vulnerability assessment criteria for rc ordinary highway bridges in Turkey", Structural Engineering and Mechanics, 43(1), 127-145.

Bezerra, F. H. R., Nascimento, A. F., Ferreira, J. M., Nogueira, F. C., Fuck, R. A., Neves, B. B. and Sousa, M. O. L. (2011), "Review of active faults in the Borborema Province, Intraplate South America – Integration of seismological and paleoseismological data", Tectonophysics, 510(3-4), 269-290.

Budnitz, R.J., Apostolakis, G., Boore, D.M., Cluff, L.S., Coppersmith, K.J., Cornell, C.A. and Morris, P.A. (1997), "Recommendations for probabilistic seismic hazard analysis: guidance on uncertainty and use of experts", U.S. Nuclear Regulatory Commission, U.S. Department of Energy, Eletric Power Research Institute, Tech. Rep. NUREG/CR-6372, U.S.

Cavalcante, G.H.F., Pereira, E.M.V., Rodrigues, I.D., Vieira Júnior, L.C.M., Padgett, J.E. and Siqueira, G.H. (2021), "Proposal of representative portfolios for federal highway bridges in Northeastern Brazil", arXiv preprint arXiv:2018.00934.

Cavalcante, G.H.F., Pereira, E.M.V, Rodrigues, I.D., Vieira Júnior, L.C.M. and Siqueira, G.H. (2023), "A new methodology to assess the structural capacity of bridge portfolios: application in Northeastern Brazilian bridges", IBRACON Struct. Mater. J., 16(1), e16101.

Chang, G.A. and Mander, J.B. (1994), "Seismic energy based fatigue damage analysis of bridge columns: Part 1 – Evaluation of seismic capacity", National Center for Earthquake Engineering Research, NY, U.S., Tech. Rep. NCEER-94-006.

Choi, E. (2002). Seismic analysis and retrofit of Mid-America bridges, Ph.D. Thesis, Georgia Institute of Technology, U.S.

Choi, E. and Jeon, J.C. (2003), "Seismic fragility of typical bridges in moderate seismic zone", KSCE Journal of Civil Engineering, 7(1), 41-51.

California Department of Transportation (2004), Caltrans Seismic Design Criteria version 1.3. Sacramento, U.S.

Federal Emergency Management Agency – FHWA (1995), "Seismic retrofitting manual for highway bridges", U.S., Tech. Rep. FHWA-RD-94-052.

Federal Emergency Management Agency – FEMA (1997), Earthquake loss estimation methodology, HAZUS-MH 2.1: Techinical Manual. Washington, DC.

Filippou, F.C., Bertero, V.V. and Popov, E.V. (1983), "Effects of bond deterioration on hysteretic behavior of reinforced concrete joints", Earthquake Engineering Research Center, University of California, Berkeley, U.S., Tech. Rep. NSF/CEE-83032.

Giardini, D., Basham, P. and Bery, M. (1999), "The global seismic hazard assessment program (GSHAP) – 1992/1999", Istituto Nazionale di Geofisica e Vulcanologia, 42(6), 957-974.

Instituto Brasileiro de Geografia e Estatística (2010), Censo Brasileiro de 2010. Rio de Janeiro, Brazil.

Jalayer, F., Beck, J.L. and Zareian, F. (2012), "Analyzing the sufficiency of alternative scalar and vector intensity measures of ground shaking based on information theory", Journal of Engineering Mechanics, 138(3), 307-3016.

Jeon, J-S., Park, J-H. and DesRoches, R. (2015), "Seismic fragility of lightly reinforced concrete frames with masonry infills", Earthquake Engineering & Structural Dynamics, 44(11), 1783-1803.

Karim, K.R. and Yamazaki, F. (2003), "A simplified method of constructing fragility curves for highway bridges", Earthquake Engineering & Structural Dynamics, 32(10), 1603-1626.

Kelly, J.M. (1993), Earthquake-Resistant Design with Rubber, (2th Edition), U.S.: Springer (California).

Lee, S.M., Kim, T.J. and Kang, S.L. (2007), “Development of fragility curves for bridges in Korea”, KSCE Journal of Civil Engineering, 11(3), 165-174.

Liao, W-I., and Loh, C-H. (2004), “Preliminary study on the fragility curves for Highway bridges in Taiwan”, Journal of the Chinese Institute of Engineers, 27(3), 367-375.

Luco, N. and Cornell, C.A. (2007), “Structure-specific scalar intensity measures for near-source and ordinary earthquake ground motions”, Earthquake Spectra, 23(2), 357-392.

Mangalathu, S., Soleimani, F. and Jeon, J-S. (2017), “Bridge classes for regional seismic risk assessment: Improving hazus models”, Engineering Structures, 148(1), 755-766.

Martin, G.R. and Yan, L. (1995), “Modeling passive earth pressure for bridge abutments”, ASCE 1995 Annual National Convention, San Diego, U.S.

Mckay, M.D., Beckman, R.J. and Conover, W.J. (1979), “Comparison of three methods for selecting values of input variables in the analysis of output from a computer code”, Technometrics, 21(2), 239-245.

McKenna F. (2011), “OpenSees: A framework for earthquake engineering simulation”, Computing in Science & Engineering, 13(4), 58-66.

Medina, A. R. and Krawinkler, H. (2004), “Seismic demands for nondeteriorating frame structures and their dependence on ground motions”, Pacific Earthquake Engineering Research Center, CA, U.S., PEER Rep. 2003/15.

Mirza, S.A. and MacGregor, J.G. (1979), “Variability of mechanical properties of reinforcing bars”, Journal of Structural Division, 105(5), 921-937.

Montgomery, D. (2017), Design and Analysis of Experiments, (8th Edition), U.S.: John Wiley & Sons (New York).

Moschonas, I.F., Kappos, A.J., Panetsos, P., Papadopoulos, V., Makarios, T. and Thanapoulos, P. (2009), “Seismic fragility curves for greek bridges: methodology and case studies”, Bulletin of Earthquake Engineering, 7(2), 439-468.

Muthukumar, S. (2003). A contact element approach with hysteresis damping for the analysis and design of pounding in bridges, Ph.D. Thesis, Georgia Institute of Technology, U.S.

Nielson, G.R. (2005), “Analytical fragility curves for highway bridges in moderate seismic zones”, Ph.D. Thesis, Georgia Institute of Technology, U.S.

Nielson, G.R. and DesRoches, R. (2007a), “Analytical seismic fragility curves for typical bridges in the Central and Southeastern United States”, Earthquake Spectra, 23(3), 615-633.

Nielson, G.R. and DesRoches, R. (2007b), “Seismic fragility methodology for highway bridges using a component level approach”, Earthquake Engineering and Structural Dynamics, 36(6), 823-839.

Nogueira, C.G. (2010). Development of mechanical, reliability and optimization models for application in reinforced concrete, Ph.D. Thesis (in Portuguese), Universidade de São Paulo, Brazil.

Novak, M. (1991), “Piles under dynamic loads”, Second International Conference on Recent Advances in Geotechnical Earthquake Engineering and Soil Dynamics, Missouri, U.S.

Oliveira, C.B.L, Greco, M. and Bittencourt, T.N. (2019), “Analysis of the Brazilian federal bridge inventory”, IBRACON Struct. Mater. J., 12(1), 1-13.

Pacific Earthquake Engineering Research Center – PEER (2021) PEER Ground Motion Database. Accessed: Jan. 26, 2021. Available: https://ngawest2.berkeley.edu/.

Padgett, J.E., and DesRoches, R. (2008), “Methodology for the development of analytical fragility curves for retrofitted bridges”, Earthquake Engineering & Structural Dynamics, 37(8), 1157-1174.

Padgett, J.E. and DesRoches, R. (2009), “Retrofitted bridge fragility analysis for typical classes of multispan bridges”, Earthquake Spectra, 25(1), 117-141.

Padgett, J.E., Nielson, B.G. and DesRoches, R. (2008), “Selection of optimal intensity measures in probabilistic seismic demand models of highway bridge portfolios”, Earthquake Engineering & Structural Dynamics, 37(5), 711-725.

Pahlavan, H., Zakeri, B., Amiri, G.G. and Shaianfar, M. (2016), “Probabilistic vulnerability assessment of horizontally curved multiframe RC box-girder highway bridges”, Journal of Performance of Constructed Facilities, 30(3), 04015038.

Petersen, M.D., Harmsen, S.C., Jaiswal, K.S., Rukstales, K.S., Lucco, N., Haller, K.M., Mueller, C.S. and Shumway, A.M. (2018), “Seismic hazard, risk, and design for South America”, Bulletin of the Seismological Society of America, 108(2), 781-800.

Santiago, W. and Beck, A. (2017), “A new study of Brazilian concrete strength conformance”, IBRACON Struct. Mater. J., 10(4), 906-923.

Santos, S.H. and Lima, S.S. (2005), “Elements for a future brazilian standard for seismic resistance of concrete structures of buildings”, IBRACON Struct. Mater. J., 1(1), 47-62.

Schrage, I. (1981), “Joint sealing and bearing systems for concrete structures”, American Concrete Institute Niagra Falls, NY, U.S.

Siqueira, G.H., Sanda, A.S., Paultre, P. and Padgett, J.E. (2014a), “Fragility curves for isolated bridges in eastern Canada using experimental results”, Engineering Structures, 74(1), 311-324.

Siqueira, G.H., Tavares, D.H., Paultre, P. and Padgett, J.E. (2014b), “Performance evaluation of natural rubber seismic isolators as a retrofit measure for typical multi-span concrete bridges in eastern Canada”, Engineering Structures, 74(1), 300-310.

Souza, B.R.S., Felipe, M.L.C., Nóbegra, P.G.B. and Nóbegra, S.H.S. (2019), “On the generation of hazard maps and response spectrum by the use of probabilistic seismic hazard analysis”, XL Ibero-Latin American Congress on Computational Methods in Engineering, Brazil.

Stewart, J.P., Midorikawa, S., Graves, R.W., Khodaverdi, K., Kishida, T., Miura, H., Bozorgnia, Y. and Campbell, K.W. (2013), “Implications of the Mw9.0 Tohoku-Oki earthquake for ground motion scaling with source, path, and site parameters”, Earthquake Spectra, 29(1), S1-S21.

Suescun, J.R. (2010). Fragility curves for bridges in Québec accounting for soil-foundation system, M.Sc. Dissertation, Université de Sherbrooke, Canada.

Tavares, D.H., Padgett, J.E. and Paultre, P. (2012), “Fragility curves of typical as-built highway bridges in eastern Canada”, Engineering Structures, 40(1), 107-118.

Wu, C.F.J. and Hamada, M.S. (2009), Experiments: Planning, Analysis, and Optimization, (2nd Edition), U.S.: John Wiley & Sons (New York).